The effects of spatial filtering and artifacts on electrocorticographic signals

2015 J. Neural Eng. 12 056008

(http://iopscience.iop.org/1741-2552/12/5/056008)

IOP Publishing

Journal of Neural Engineering

J. Neural Eng. 12 (2015) 056008 (10pp)

doi:10.1088/1741-2560/12/5/056008

The effects of spatial filtering and artifacts on electrocorticographic signals

Y Liu[1,2,*], W G Coon[2,3,*], A de Pesters[2,3], P Brunner[2,4] and G Schalk[2,3,4]

[1] School of Mechanical Engineering, Beijing Institute of Technology, Beijing, People's Republic of China
[2] National Center for Adaptive Neurotechnologies, Wadsworth Center, New York State Department of Health, Albany, NY, USA
[3] Department of Biomedical Sciences, State University of New York at Albany, Albany, NY, USA
[4] Department of Neurology, Albany Medical College, Albany, NY, USA

E-mail: gschalk@neurotechcenter.org

Received 23 February 2015, revised 1 July 2015
Accepted for publication 14 July 2015
Published 13 August 2015

CrossMark

Abstract

Objective. Electrocorticographic (ECoG) signals contain noise that is common to all channels and noise that is specific to individual channels. Most published ECoG studies use common average reference (CAR) spatial filters to remove common noise, but CAR filters may introduce channel-specific noise into other channels. To address this concern, scientists often remove artifactual channels prior to data analysis. However, removing these channels depends on expert-based labeling and may also discard useful data. Thus, the effects of spatial filtering and artifacts on ECoG signals have been largely unknown. This study aims to quantify these effects and thereby address this gap in knowledge. *Approach*. In this study, we address these issues by exploring the effects of application of two types of unsupervised spatial filters and three methods of detecting signal artifacts using a large ECoG data set (20 subjects, four task conditions in each subject). *Main results*. Our results confirm that spatial filtering improves performance, i.e., it reduces ECoG signal variance that is not related to the task. They also show that removing artifactual channels automatically (using quantitatively defined rejection criteria) or manually (using expert opinion) does not increase the total amount of task-related information, but does avoid potential contamination from one or more noisy channels. Finally, applying a novel 'median average reference' filter does not require the elimination of artifactual channels prior to spatial filtering and still mitigates the influence of channels with channel-specific noise. Thus, it allows the investigator to retain more potentially useful task-related data. *Significance*. In summary, our results show that appropriately designed spatial filters that account for both common noise and channel-specific noise greatly improve the quality of ECoG signal analyses, and that artifacts in only a single channel can result in profound and undesired effects on all other channels.

Keywords: electrocorticography, spatial filtering, common average reference, signal artifact

(Some figures may appear in colour only in the online journal)

1. Introduction

In recent years, there has been increased interest in electrocorticographic (ECoG) signals, which are recorded directly from the surface of the brain. ECoG signals are attractive for research because they have a much higher signal-to-noise ratio (SNR) than noninvasive recording methods such as scalp-recorded electroencephalography. However, even ECoG signals are susceptible to noise. This noise can conveniently be divided into two different types: (1) noise that is common to all channels (e.g., noise introduced by the signal reference), and (2) noise that is unique to a particular channel

* Authors contributed equally to this work.

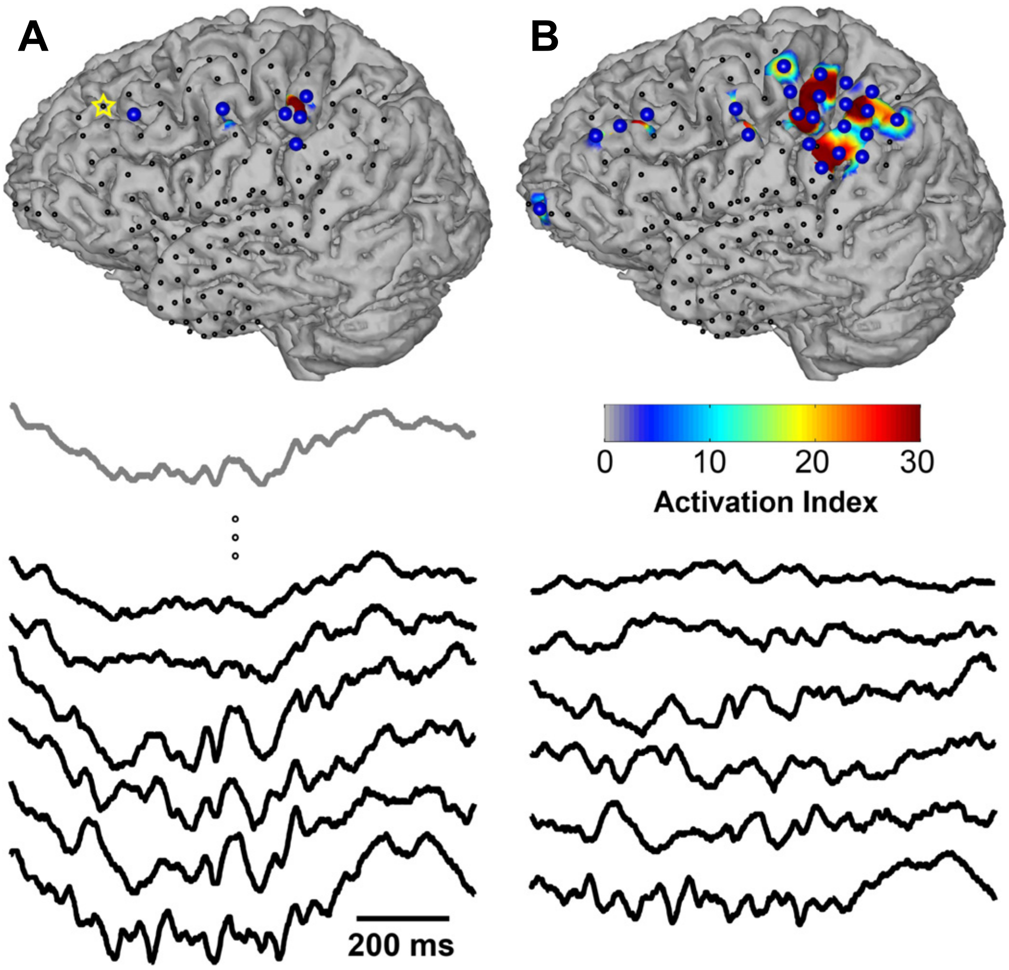

Figure 1. Using a common average reference (CAR) filter improves the relationship between ECoG signals and a motor task. Blue/small black circles indicate which electrode locations did/did not hold signals that were significantly modulated by a motor task, respectively. The activation indices (i.e., negative logarithm of *p*-values associated with the correlation between the ECoG broadband gamma signals and the task) are color-coded and rendered on the cortical surface (see methods for details on signal processing and visualization/rendering). (A): results that were derived without any spatial filtering. Black traces show representative unfiltered signals from channels with low-frequency noise components. The gray trace shows the average of the black traces, i.e., an estimate of the underlying common noise. The star in the topography indicates the reference electrode used at time of data acquisition (same in (B)). (B): results that were derived when using a common average reference (CAR) filter (i.e., the gray common average trace was subtracted from each signal). In (B), more locations are statistically modulated by the task compared to (A).

(e.g., noise introduced by a broken wire). Our ability to extract task-related information from ECoG data sets is affected by both sources of noise.

Common noise (source 1) is usually either ignored (Pistohl *et al* 2008, Anderson *et al* 2012, Flamary and Rakotomamonjy 2012, Flint *et al* 2012, Liang and Bougrain 2012) or addressed by re-referencing to a common signal average, a procedure most often referred to as spatial filtering in the ECoG literature (Schalk *et al* 2007, Brunner *et al* 2009, Ganguly *et al* 2009, Gunduz *et al* 2009, 2012, Kubanek *et al* 2009, Acharya *et al* 2010, Chao *et al* 2010, Pei *et al* 2011, Wang *et al* 2011, 2012, Miller *et al* 2012, Potes *et al* 2012). These spatial filters are typically referred to as common average reference (CAR) filters. While systematic studies that investigated the effect of signal contamination on ECoG signals have been scarce (Ball *et al* 2009), it is widely believed that spatial filters improve the SNR in ECoG signals, and hence allow investigators to make more specific statements about the relationship of these ECoG signals with relevant task parameters (see figure 1 for an example).

Channel-specific noise (source 2) is often addressed by simply removing noisy channels from analyses. In this context, it is important to recognize that there is a balance between the detrimental effect of artifacts and the beneficial effect of task-related information contained within a given channel—this balance and the nature of the research question at hand will determine the extent to which removing artifactual channels will be beneficial overall. In addition, identification of such noisy channels is inherently subjective and depends on the availability of an expert. However, appropriate identification of these noisy channels is critical, as their inclusion may not only lower the SNR ratio of the analyses but also inject spurious task-related effects (i.e., a signal artifact) into a large number of channels (figure 2). This effect

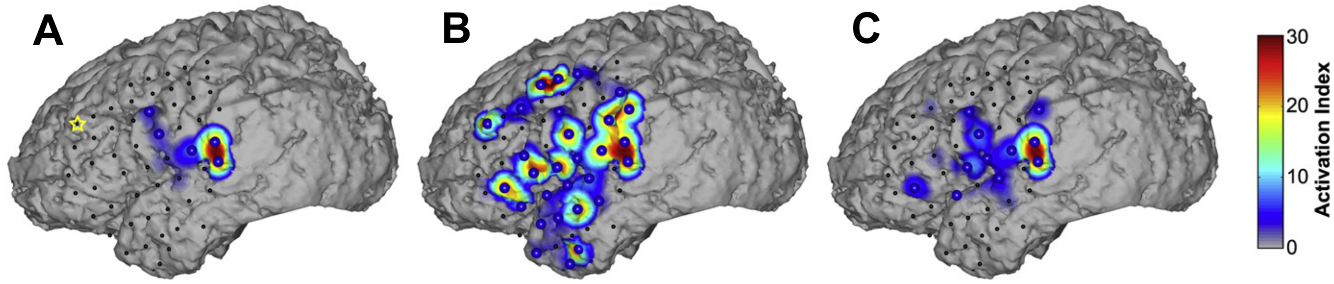

Figure 2. A single noisy channel can introduce spurious task-related signals into an entire data set. In this example, one channel contains very few samples that are very large outliers (see traces in figure 8(B)). These outliers create a spurious task-related correlation. (A): when no spatial filter is applied, ECoG signals in several locations show correlations with a passive listening task. These locations (in posterior parts of the superior temporal gyrus) are consistent with expectations based on prior research. (Dots/colors and reference electrode are shown as in figure 1.) (B): using a CAR filter that includes the noisy channel can introduce the channel-specific noise (e.g., the few outlier samples in this example) into all other channels, and thus lead to spurious activations in many locations across wide areas of the brain that are not believed to participate in processing auditory stimuli. (C): by using a CAR filter that excludes the noisy channel, one can avoid the problem in figure 2(B) and identify additional locations with task-related information. See methods for details on the task, and signal processing and rendering procedures.

has serious and undesired consequences for scientific interpretation, but has not received formal attention in the ECoG literature. Efforts to address signal contamination with more sophisticated techniques such as adaptive or supervised spatial filters have yielded promising results in certain contexts (Marathe and Taylor 2013), but these approaches are often impractical as they require previous knowledge about task parameters or come with their own limitations when interpreting neuroscientific results (Haufe *et al* 2014). Accordingly, unsupervised, non-adaptive spatial filters are often preferable despite their relatively unknown efficacy.

In this study, we evaluated the effects of two types of unsupervised spatial filters and three methods to identify noisy channels on a large ECoG data set (20 subjects, four tasks). The results show that the addition of a spatial filter greatly improves results. Specifically, the results for both a mean and a novel median CAR filter significantly outperform the results when no spatial filter is applied (63.4% and 84.4% average improvement over no spatial filter, respectively). We show that removing channel-specific noise automatically by using reasonable, quantitatively defined rejection criteria, or manually by using expert opinion, does not overall increase the total amount of task-related information. More importantly, we show that excluding channels in these ways can avoid potential task-related contamination from one or a few particularly noisy channels. Finally, we find that a median average reference filter can be applied to all channels (including those with channel-specific noise) and will mitigate the influence of those noisy channels while also allowing the investigator to retain the potentially task-related signals contained in those channels.

2. Methods

2.1. Subjects

Subjects included in this study were twenty patients with intractable epilepsy who underwent temporary placement of subdural electrode arrays to localize seizure foci prior to surgical resection. Table 1 summarizes the subjects' clinical profiles. All gave informed consent for this study, which was approved by the Institutional Review Board of Albany Medical College. Electrode grids consisted of platinum-iridium electrodes that were 4 mm in diameter (2.3 mm exposed), embedded in silicone, and spaced with an inter-electrode distance of 1 cm. Grid placement and duration of ECoG monitoring were based solely on the requirements of the clinical evaluation, without any consideration of this study. Following placement of the subdural grid, each subject had postoperative anterior-posterior and lateral radiographs, as well as computerized tomography (CT) imaging, to identify grid locations. Figure 3 shows locations of recorded electrodes (shown as small black dots) from all 20 subjects, projected onto the standard Montreal Neurological Institute (MNI) brain model and separately for right and left hemisphere.

2.2. Experimental paradigm

Each subject performed alternating sequences of repetitive movements of the hand (manipulating a Rubik's cube) or orofacial muscles (protruding and retracting the tongue or lips), passive listening (short stories presented with computer speakers), and periods of rest. See figure 4 for a diagram of this experiment. Each subject was visually cued by the words 'solve Rubik's cube', 'stick out tongue', 'kiss', 'listen carefully', or 'stop and relax'. Each task was performed for 15 s (17–36 s for passive listening, depending on which narrative was presented). The motor tasks were performed at a self-paced rate of about two repetitions per second. Each task was followed by a resting period of 15 s before the next task proceeded. One run consisted of 5 repetitions of this sequence over the course of 10.22 min (4.75 rest, 1.25 hand moving, 1.25 tongue moving, 1.25 lips moving, and 1.72 min passive listening). We typically recorded one initial run to familiarize the subject with the task. All analyses in this article are for one run following the initial training run.

Table 1. Clinical profiles of the 20 subjects. All subjects had normal cognitive capacity and were literate and functionally independent. Language lateralization (LL) was based on the Wada test. '# of elec.' refers to the number of electrode contacts on each implanted grid or strip.

Subject	Age	Sex	Handedness	LL	Seizure focus	Grid/Strip location	# of elec.
A	36	F	R	L	Right temporal	Right frontal	40
						Right temporal	24
B	24	M	R	L	Right temporal	Right frontal	64
						Right temporal	33
C	29	F	R	L	Left temporal	Left fronto-parietal	64
						Left temporal	23
						Left temporal pole	3
						Left occipital	6
D	30	M	R	L	Left temporal	Left frontal	40
						Left temporal	35
						Left temporal pole	4
						Left occipital	4
E	29	F	R	L	Left temporal	Left frontal	56
						Left temporal	35
						Left temporal pole	4
						Left orbital pole	6
F	18	M	R	Bilateral	Left frontal	Left frontal	78
						Left frontal pole	6
G	26	F	R	L	Left temporal	Left frontal	64
						Left temporal	35
						Left temporal pole	4
						Left occipital	6
H	56	M	R	L	Left temporal	Left frontal	56
						Left temporal	35
						Left occipital	6
I	24	M	R	L	Left frontal	Left frontal	64
						Left frontal pole	12
J	23	M	R	L	Right temporal	Right frontal	64
						Right temporal	35
						Right frontal pole	6
						Right occipital	6
K	25	M	R	L	Right frontal	Right frontal	64
						Right parietal	28
						Right temporal	8
						Right orbital	4
L	45	M	R	L	Left temporal	Left fronto-temporal	54
						Left temporal pole	4
M	49	F	L	NA	Left temporal	Left frontal	41
						Left temporal	24
						Left temporal pole	4
						Left superior temporal	6
N	52	M	L	L	Left parietal	Left fronto-parietal	64
O	29	F	R	Bilateral	Left temporal	Left frontal	40
						Left temporal	68
						Left temporal pole	4
						Left orbital pole	4
						Left occipital	4
P	45	F	L	L	Left temporal	Left frontal	31
						Left temporal	27
Q	60	M	R	NA	Left temporal	Left temporal	17
						Left parieto-occipital	42
R	14	F	R	NA	Right frontal	Right frontal	49
						Right superior temporal	6
S	28	M	R	L	Left temporal	Left frontal	52
						Left temporal	66
						Left parietal	16
T	25	F	R	L	Left temporal	Left frontal	16

Table 1. (Continued.)

Subject	Age	Sex	Handedness	LL	Seizure focus	Grid/Strip location	# of elec.
						Left temporal	66

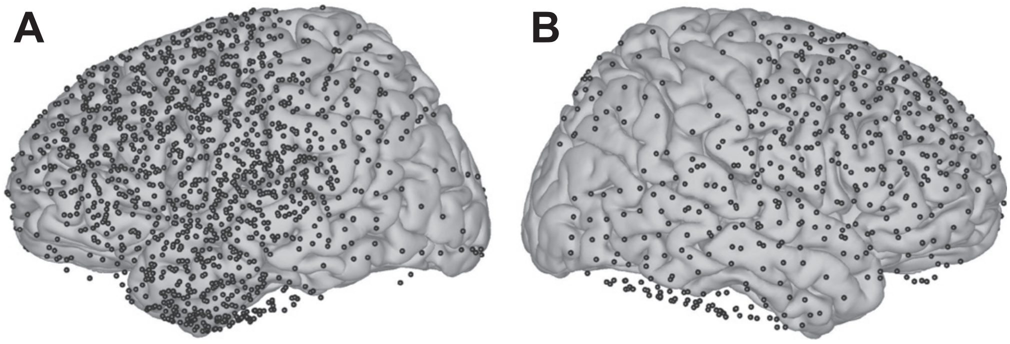

Figure 3. Locations of recorded electrodes from all 20 subjects, projected onto the standard MNI brain model. (A): electrodes from the 15 subjects with electrodes on the left hemisphere. (B): electrodes from the five subjects with electrodes on the right hemisphere.

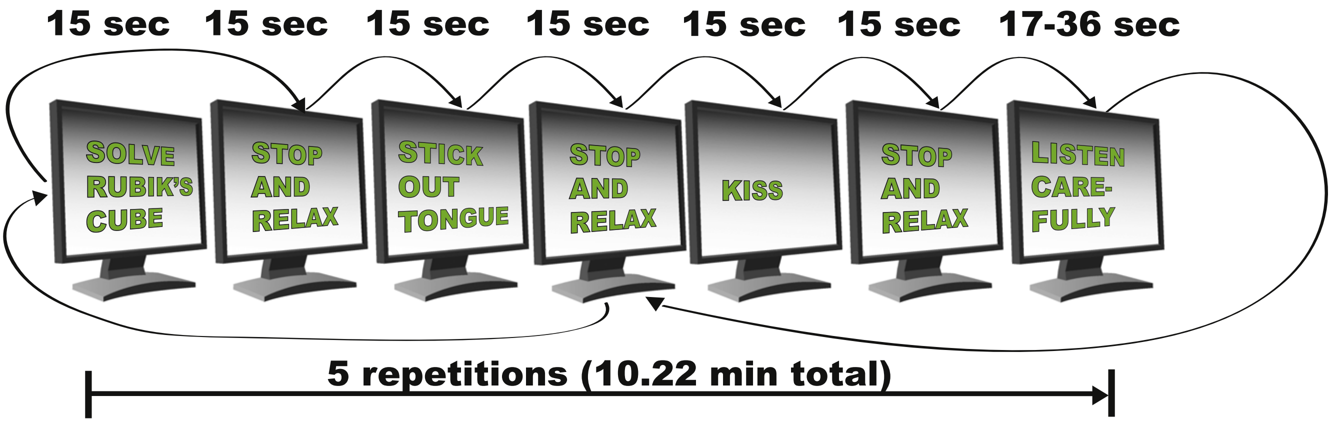

Figure 4. Experimental setup. Subjects followed instructions displayed on computer monitors in front of them. They alternated between task and rest (baseline) conditions while ECoG signals were simultaneously recorded. Each of the four task conditions was repeated five times, for a total task run time of 10.2 min.

2.3. Data collection

We acquired ECoG signals from 58–134 electrodes using g.USBamp or g.HIamp biosignal acquisition devices (g.tec, Graz, Austria). These devices employed anti-aliasing filters, used sample-and-hold to deliver synchronous (no-phase-delay) readouts, and provided data at a rate of 1 200 Hz. Data acquisition, storage and stimulus presentation were accomplished using the BCI2000 software package (Schalk *et al* 2004, Mellinger *et al* 2007, Schalk and Mellinger 2010).

2.4. Cortical mapping

We used Curry software (Neuroscan, El Paso, TX) to create subject-specific three-dimensional (3D) cortical brain models from high-resolution pre-operative magnetic resonance imaging (MRI) scans. We co-registered the MRIs with post-operative CT images and extracted, for each grid electrode, the stereotactic coordinates and functional area according to the Talairach atlas (Lancaster *et al* 2000). We used the 3D cortical template provided by the MNI to display aggregate electrode locations from multiple subjects onto a common coordinate space. Finally, we projected electrodes onto subject-specific brain models to render activation maps using our NeuralAct software package (Kubanek and Schalk 2014). Briefly, to compute activation maps, the activation index value for each electrode location was spatially convolved with a linear decay spatial kernel whose value reached zero at the interelectrode distance (10 mm in this study). Thus, maps are the result of linear interpolations at locations between the electrodes.

2.5. Spatial filter design

One goal of our study was to compare different spatial filtering methods with regard to their ability to remove spatial noise. To do this, we used the following signal pre-processing and feature extraction methods: first, we removed all frequencies below 5 Hz from the ECoG signals with a high-pass filter. Then, we implemented three spatial filter conditions (no CAR, mean CAR, and median CAR) and three channel exclusion conditions (no channel exclusion, automatic (based on criteria described below) or manual (based on expert opinion)), for a total of seven different spatial filter conditions (see section 3.1 for more details on spatial filter conditions). To implement mean CAR filters, we obtained the CAR-filtered signal s_h' at channel h using $s_h' = s_h - \frac{1}{H}\sum_{q=1}^{H} s_q$. s_h was the original signal sample at a particular time. For mean CAR filters that included all channels, H was the total number of channels in that subject. For mean CAR filters that excluded channels, H was the number of channels remaining after removing noisy channels. We implemented median CAR filters similarly, by obtaining the filtered signal s_h' at channel h using s_h minus the median value of all signal samples (instead of the mean). Next, ECoG signals from each channel were band-pass filtered in the broadband gamma frequency band (70–170 Hz), because activity in this frequency band has been shown in many previous ECoG studies to be an accurate measure of task-related activity (Miller *et al* 2007, Schalk *et al* 2007, Sinai *et al* 2009, Pei *et al* 2011, Pasley *et al* 2012). We then estimated broadband gamma power by extracting the amplitude envelope of activity in the broadband gamma band using the Hilbert transform, low-pass filtered (moving average with a 150 ms window width), and downsampled to 10 Hz before submitting the resulting broadband gamma power estimates to subsequent analyses.

2.6. Channel exclusion methods

We identified noisy channels (to be excluded from spatial filters) based on either expert opinion (manual selection) or one of three quantitative rejection criteria (automatic selection). These rejection criteria identified channels with abnormal amplitude distributions, excessive line noise, or outlier data points. To identify channels with abnormal amplitude distributions, we log-transformed the root mean square of the raw voltage values (RMSVs) for all channels and normalized them by calculating z-scores. We then calculated p-values using a Gaussian distribution that was fitted to the data and excluded a channel if its mean amplitude was statistically significantly different from the mean amplitude of all other channels ($p < 0.05$). To identify channels with excessive line noise, we calculated a SNR by dividing the power (calculated using the fast Fourier transform) at each channel's line noise frequency (60 Hz) by the median amount of line noise (i.e., 60 Hz power) across all channels in that subject. We again fit a Gaussian to this distribution of SNR values, obtained p-values from this Gaussian, and excluded channels with statistically significant deviations from the average amount of noise across all channels ($p < 0.01$). To identify channels with outliers, for each channel's raw signals, we defined outlier thresholds of greater than ten standard deviations below or above the raw signal values' 2nd and 98th percentiles, respectively. We then excluded channels that contained at least one data point that exceeded either of these thresholds. Figure 5 shows some time courses, spectra, and amplitude distributions from a typical ECoG signal channel (figure 5(A)) and from channels with significant deviations in signal amplitude and line noise (figure 5(B)), or outliers (figure 5(C)).

2.7. Detection of task-related cortical locations

To determine the cortical locations that were related to each of the four tasks (movement of the hand, tongue, lips, and passive listening), we first calculated, separately for each task and location, the pairwise Spearman's correlation coefficient (Spearman's rho, hereafter referred to as 'r') between task labels (i.e., task and rest) and broadband gamma power. We then created a surrogate data set by destroying the temporal relationship between broadband gamma power values and task labels before recalculating the correlation. We did this by randomly shuffling the task labels for each sample (i.e. sample-by-sample randomization). Similar to (Schalk *et al* 2007), we repeated this operation 250 times and obtained a Gaussian distribution of correlation coefficients. We then compared the one true correlation coefficient to the Gaussian surrogate to derive a significance level (p-value). For locations with significant correlation coefficients (i.e., $p < 0.001$ after Bonferroni correction), we projected the negative logarithm of the corresponding p-values (i.e., $-\log 10(p)$) onto the corresponding individual brain model. The negative logarithm of the p-value has been used in many previous studies (e.g., Schalk *et al* 2007, Kubanek *et al* 2009, Gunduz *et al* 2011) as an 'activation index' to visualize results from similar correlation analyses.

2.8. Performance metric (PM)

To quantify the performance of each spatial filter condition, we derived a PM by summing the values of squared correlation coefficients (Spearman's r^2s) from all locations with statistically significant correlation with a task (i.e., $p < 0.001$ after Bonferroni correction). Thus, the PM defined here reflects both the number of electrodes that our analyses could identify as task-related, as well as the degree of the relationship with the task. Finally, to evaluate the performance in each of our spatial filter conditions, we averaged performance values across all four task conditions.

3. Results

3.1. Quantitative results

The main results of our study are shown in figure 6, which shows a comparison of the performance of each of the seven different spatial filter conditions (i.e., no spatial filter, a mean and a median CAR filter with all channels included, a mean and a median CAR filter with noisy channels removed automatically, and a mean and a median CAR filter with noisy channels removed manually). The results demonstrate that using a spatial filter greatly improves results over not using any spatial filter: both mean and median CAR filters significantly outperformed the no spatial filter condition (63.4% and 84.4% average improvement over no spatial filter, respectively). For both mean and median CAR filters,

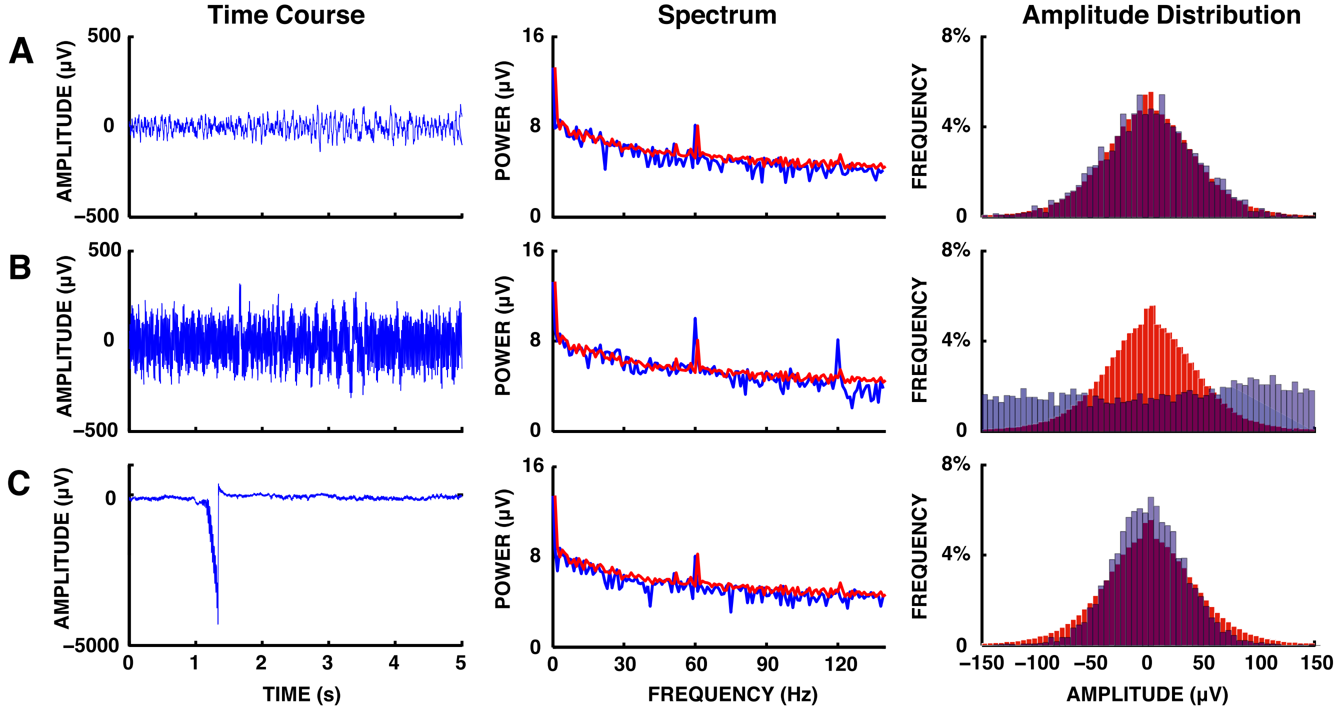

Figure 5. Different sources of signal noise. Left column: raw ECoG signal time course for three different channels. Middle and right columns: spectra and amplitude distributions of the channel shown on the left (blue traces/histograms, respectively) and of the average across all channels in that subject (red traces/histograms, respectively). (A): typical ECoG signal channel. (B): channel with a significant amount of line noise and an abnormal amplitude distribution. (C): channel with outliers.

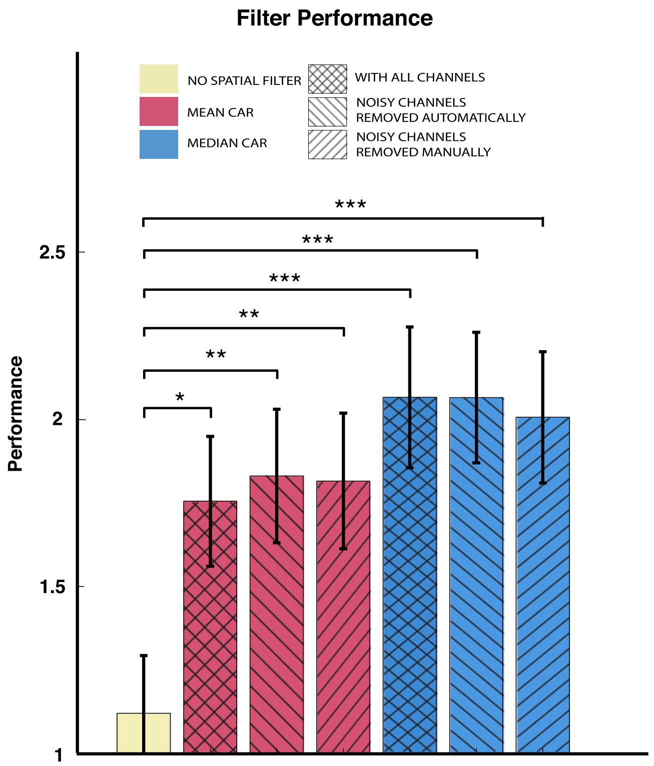

Figure 6. Comparison of the performance of different spatial filters. $p < 0.05$*; $p < 0.01$**; $p < 0.001$***.

automatic and manual exclusion of noisy channels achieved similar results.

3.2. Qualitative results

Figure 6 shows quantitative evidence that spatial filtering has a strong effect on the detection of task-related ECoG activity. Figure 7 provides qualitative examples that highlight this effect. This figure also illustrates an example of how the exclusion of noisy channels from the common average can in some cases profoundly affect the results.

3.2.1. Excluding noisy channels does not increase the total amount of task-related information. In this paper, we evaluated two methods for removing these channels: automatic removal according to quantitative rejection criteria, and manual removal by subjective expert opinion. The results for both methods are similar to when no channel was removed (figure 6). At the same time, figure 7 shows an exemplary topography from one subject who performed the lip protrusion/retraction task. Although we would expect to see task-related activations in oral motor areas, without applying a spatial filter (figure 7(A)) or removing noisy channels from this filter (figure 7(B)), such activations are not readily apparent. In contrast, when noisy channels are removed using automated/manual selection (figures 7(C),

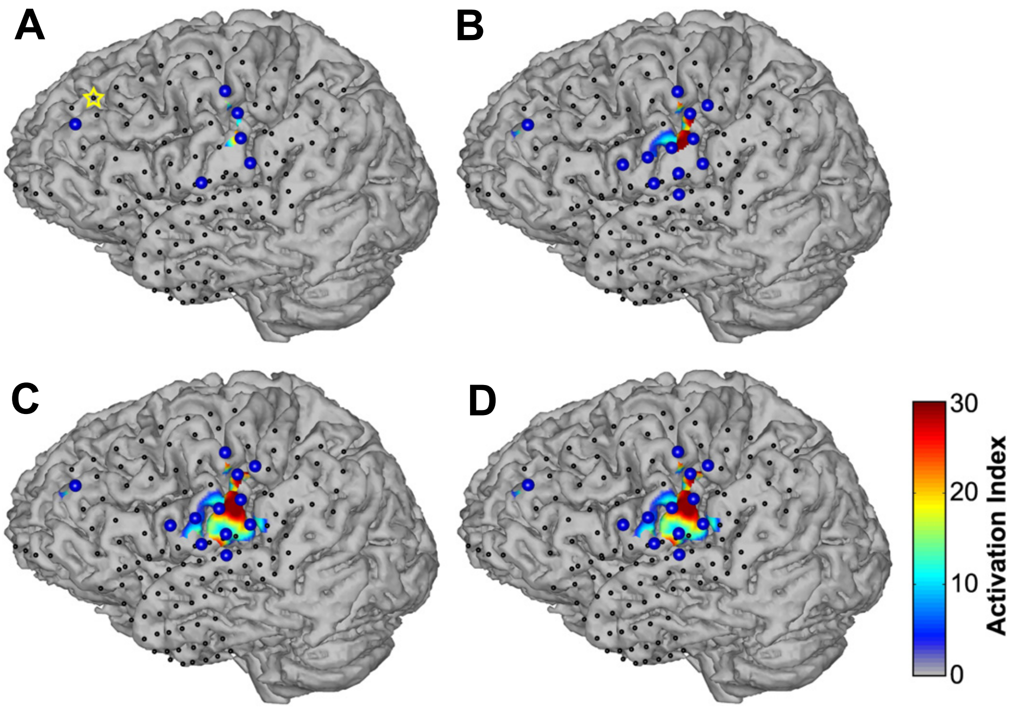

Figure 7. Excluding channels manually (based on the judgment of a human expert) yields results similar to those generated by automatic, computerized techniques (reference electrode and dots/colors are shown as in figure 1, derived from the same motor task). (A): using no spatial filter does not highlight task-related activations in oral motor (i.e., inferior posterior frontal) cortex. (B): application of a CAR filter results in somewhat higher activation indices. (C)/(D): excluding channels using computerized algorithms/expert opinion, respectively, reveals the expected activations throughout oral motor cortex.

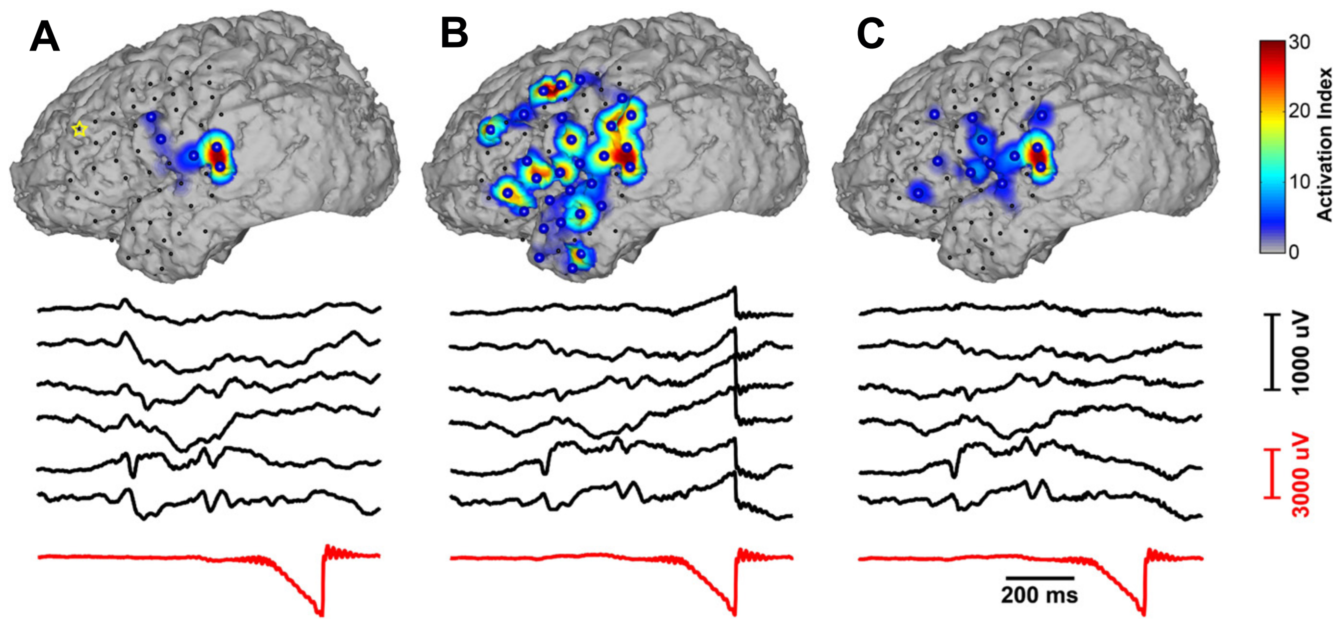

Figure 8. A median average reference filter is robust to outliers (dots/colors are shown as in figure 1, derived from a passive listening task; reference used at time of data acquisition is the same as depicted in figure 2(A)). Star shows reference electrode used at time of data acquisition. Black traces show representative signal recordings for (A)–(C), respectively. Red traces show signals recorded from the channel responsible for the effect seen in (B). (A): no spatial filtering yields physiologically plausible results with small activation indices and does not contaminate other channels with noise from the red artifactual channel. (B): using the spatial signal mean to build a CAR filter leaves the filter susceptible to signal artifacts unique to individual channels. In this case, the outliers from the red trace were introduced into all other channels by the filter, yielding seemingly task-related but (almost certainly) erroneous results (note that this is the same analysis result depicted in figure 2(B)). (C): the same analysis, using a median CAR filter. Note that these results, which include all channels, are qualitatively similar to the results shown in figure 2(C), in which a mean CAR filter is used after removing noisy channels.

(D), respectively), task-related activations in oral motor areas are apparent.

3.2.2. Applying a median average reference mitigates the effect of noisy channels. Defining noisy channels depends on the availability of an expert, is time consuming, and is subjective. In addition, since data are often scarce, exclusion of noisy channels may also discard potentially meaningful physiological information contained in those channels. Thus, there are several reasons why scientists may want to retain all or as many channels as possible. Our results show that using a median average reference filter instead of a mean average reference filter can mitigate the influence of channels with too much channel-specific noise (figure 8) while still avoiding the problem of discarding potentially useful data. Importantly, this novel spatial filter design introduced here performs equally to the more traditionally used mean CAR filter, but also allows the investigator to retain additional task-related information while simultaneously preventing one or a few noisy channels from injecting spurious signal phenomena into other channels.

4. Discussion

In this study, we explored the effects of two types of unsupervised spatial filters and three methods of addressing noisy channels on task-related analyses that were performed on a large ECoG data set (20 subjects, four task conditions). These results confirm and quantify the important effects of spatial filter application. For example, using a mean CAR filter will reduce common spatial noise. At the same time, in rare cases, a mean CAR filter can also spread artifacts from some channels into other channels. Distinguishing these two effects is difficult if not impossible, since both increase the relationship with the task and/or the number of locations that show such relationships. However, the results shown in figure 6 suggest that mean CAR filtering including all channels tends to perform worse than mean CAR filtering excluding noisy channels, and that median CAR filtering may perform better than mean CAR filtering. Thus, we conclude that spreading apparently task-related artifacts across channels can substantially affect the results, but almost certainly occurs only rarely.

Our results highlight the importance of systematic approaches to identifying those channels that should be excluded from spatial filters. They also demonstrate that, should investigators wish to include all channels in their analyses, using a median average reference filter can mitigate the influence of channels with too much channel-specific noise without discarding valuable task-related data. Nevertheless, although using a median average filter avoids many of the potential problems of the more traditional CAR filter, it does not remove the important need to visually inspect individual channels.

In contrast to most other studies, we studied not only the effect that common noise has on data analyses but also the effect that channel-specific noise can have on data analyses. Results can be worse when noisy channels are included in the most frequently used spatial filter, a mean CAR (Schalk *et al* 2007, Brunner *et al* 2009, Ganguly *et al* 2009, Gunduz *et al* 2009, Kubanek *et al* 2009, Acharya *et al* 2010, Chao *et al* 2010, Pei *et al* 2011, Wang *et al* 2011, 2012, Gunduz *et al* 2012, Hermes *et al* 2012, Miller *et al* 2012, Potes *et al* 2012). However, it is clear that the balance between the detrimental effect of artifacts and the beneficial effect of task-related information contained within a given channel will determine whether including or excluding it from a spatial filter will improve or degrade results in subsequent analyses. Unfortunately, there is no simple answer to this quandary; as the results shown in figure 6 illustrate, excluding noisy channels does not overall improve the total amount of task-related information. However, in some cases, such as when highly artifactual data points occur during only small portions of the signal (see figures 2 and 8 for an example), removing channels can clearly be beneficial. In light of this, a critical takeaway from our study is that otherwise clean channels with significant signal artifact or data point outliers can pollute entire data sets under certain conditions. These channels must be dealt with, either by removing them entirely, by removing just outlier data points, or by using alternative spatial filters that are intrinsically robust to outliers (such as the median CAR filter introduced here).

While the results of our study were derived from a large ECoG data set, the extent to which they may generalize to other data acquisition equipment, other types of tasks, or other types of analysis procedures, is currently unclear. Thus, further work will be needed to verify that the results from our study still apply to other scenarios.

In summary, the results shown in this paper demonstrate that both common noise and channel-specific noise degrade the quality of ECoG signals and can impede the extraction of task-related information from these signals if not properly addressed. Removing noisy channels from certain spatial filters (e.g., a mean CAR filter) or incorporating them into spatial filters that are robust to outliers (e.g., a median CAR filter) are both efficient means with which an investigator can address the problem of noise in ECoG signals. Future work should investigate the degree to which these findings generalize to other types of data sets and analysis approaches.

Acknowledgments

This work was supported by the Beijing Institute of Technology (3030012211438), the NIH (EB00856, EB006356 and EB018783), the US Army Research Office (W911NF-08-1-0216, W911NF-12-1-0109, W911NF-14-1-0440) and Fondazione Neurone. The authors acknowledge Marcia Sanders for her invaluable assistance in editing the manuscript.

References

Acharya S, Fifer M S, Benz H L, Crone N E and Thakor N V 2010 Electrocorticographic amplitude predicts finger positions during slow grasping motions of the hand *J. Neural Eng.* **7** 046002

Anderson N R, Blakely T, Schalk G, Leuthardt E C and Moran D W 2012 Electrocorticographic (ECoG) correlates of human arm movements *Exp. Brain Res.* **223** 1–10

Ball T, Kern M, Mutschler I, Aertsen A and Schulze-Bonhage A 2009 Signal quality of simultaneously recorded invasive and non-invasive EEG *Neuroimage* **46** 708–16

Brunner P *et al* 2009 A practical procedure for real-time functional mapping of eloquent cortex using electrocorticographic signals in humans *Epilepsy Behav.* **15** 278–86

Chao Z C, Nagasaka Y and Fujii N 2010 Long-term asynchronous decoding of arm motion using electrocorticographic signals in monkeys *Front. Neuroeng.* **3** 3

Flamary R and Rakotomamonjy A 2012 Decoding finger movements from ECoG signals using switching linear models *Front. Neurosci.* **6** 29

Flint R D, Lindberg E W, Jordan L R, Miller L E and Slutzky M W 2012 Accurate decoding of reaching movements from field potentials in the absence of spikes *J. Neural Eng.* **9** 046006

Ganguly K, Secundo L, Ranade G, Orsborn A, Chang E F, Dimitrov D F, Wallis J D, Barbaro N M, Knight R T and Carmena J M 2009 Cortical representation of ipsilateral arm movements in monkey and man *J. Neurosci.* **29** 12948–56

Gunduz A, Brunner P, Daitch A, Leuthardt E C, Ritaccio A L, Pesaran B and Schalk G 2011 Neural correlates of visual-spatial attention in electrocorticographic signals in humans *Front. Hum. Neurosci.* **5** 89

Gunduz A, Brunner P, Daitch A, Leuthardt E C, Ritaccio A L, Pesaran B and Schalk G 2012 Decoding covert spatial attention using electrocorticographic (ECoG) signals in humans *Neuroimage* **60** 2285–93

Gunduz A, Sanchez J C, Carney P R and Principe J C 2009 Mapping broadband electrocorticographic recordings to two-dimensional hand trajectories in humans motor control features *Neural Netw.* **22** 1257–70

Haufe S, Meinecke F, Görgen K, Dähne S, Haynes J D, Blankertz B and Bießmann F 2014 On the interpretation of weight vectors of linear models in multivariate neuroimaging *Neuroimage* **87** 96–110

Hermes D, Siero J C, Aarnoutse E J, Leijten F S, Petridou N and Ramsey N F 2012 Dissociation between neuronal activity in sensorimotor cortex and hand movement revealed as a function of movement rate *J. Neurosci.* **32** 9736–44

Kubanek J, Miller K, Ojemann J, Wolpaw J and Schalk G 2009 Decoding flexion of individual fingers using electrocorticographic signals in humans *J. Neural Eng.* **6** 066001

Kubanek J and Schalk G 2014 NeuralAct: a tool to visualize electrocortical (ECoG) activity on a three-dimensional model of the cortex *Neuroinformatics* **13** 167–74

Lancaster J L, Woldorff M G, Parsons L M, Liotti M, Freitas C S, Rainey L, Kochunov P V, Nickerson D, Mikiten S A and Fox P T 2000 Automated Talairach atlas labels for functional brain mapping *Hum. Brain Mapp.* **10** 120–31

Liang N and Bougrain L 2012 Decoding finger flexion from band-specific ECoG signals in humans *Front. Neurosci.* **6** 91

Marathe A and Taylor D 2013 Decoding continuous limb movements from high-density epidural electrode arrays using custom spatial filters *J. Neural Eng.* **10** 036015

Mellinger J and Schalk G 2007 *Toward Brain-Computer Interfacing* ed G Dornhege, J del, R Millan, T Hinterberger, D McFarland and K Müller (Cambridge, MA: MIT Press) pp 359–67

Miller K J, Hermes D, Honey C J, Hebb A O, Ramsey N F, Knight R T, Ojemann J G and Fetz E E 2012 Human motor cortical activity is selectively phase-entrained on underlying rhythms *PLoS Comp. Biol.* **8** e1002655

Miller K J, Leuthardt E C, Schalk G, Rao R P, Anderson N R, Moran D W, Miller J W and Ojemann J G 2007 Spectral changes in cortical surface potentials during motor movement *J. Neurosci.* **27** 2424–32

Pasley B N, David S V, Mesgarani N, Flinker A, Shamma S A, Crone N E, Knight R T and Chang E F 2012 Reconstructing speech from human auditory cortex *PLoS Biol.* **10** e1001251

Pei X, Barbour D L, Leuthardt E C and Schalk G 2011 Decoding vowels and consonants in spoken and imagined words using electrocorticographic signals in humans *J. Neural Eng.* **8** 046028

Pistohl T, Ball T, Schulze-Bonhage A, Aertsen A and Mehring C 2008 Prediction of arm movement trajectories from ECoG-recordings in humans *J. Neurosci. Methods* **167** 105–14

Potes C, Gunduz A, Brunner P and Schalk G 2012 Dynamics of electrocorticographic (ECoG) activity in human temporal and frontal cortical areas during music listening *Neuroimage* **61** 841–8

Schalk G, Kubanek J, Miller K, Anderson N, Leuthardt E, Ojemann J, Limbrick D, Moran D, Gerhardt L and Wolpaw J 2007 Decoding two-dimensional movement trajectories using electrocorticographic signals in humans *J. Neural Eng.* **4** 264

Schalk G, McFarland D J, Hinterberger T, Birbaumer N and Wolpaw J R 2004 BCI2000: a general-purpose brain-computer interface (BCI) system *IEEE Trans. Biomed. Eng.* **51** 1034–43

Schalk G and Mellinger J 2010 *A Practical Guide to Brain-Computer Interfacing with BCI2000* 1st edn (London, UK: Springer)

Sinai A, Crone N, Wied H, Franaszczuk P, Miglioretti D and Boatman-Reich D 2009 Intracranial mapping of auditory perception: event-related responses and electrocortical stimulation *Clin. Neurophysiol.* **120** 140–9

Wang Z, Gunduz A, Brunner P, Ritaccio A L, Ji Q and Schalk G 2012 Decoding onset and direction of movements using electrocorticographic (ECoG) signals in humans. *Front. Neuroeng.* **5** 15

Wang Z, Ji Q, Miller K and Schalk G 2011 Prior knowledge improves decoding of finger flexion from electrocorticographic signals *Front. Neurosci.* **5** 127